Gramicidin A as a mechanical sensor for mixed nonideal lipid membranes

Oleg V. Kondrashov* and Sergey A. Akimov†
A.N. Frumkin Institute of Physical Chemistry and Electrochemistry, Russian Academy of Sciences, 31/4 Leninskiy prospekt, Moscow 119071, Russia

(Received 23 August 2023; revised 16 April 2024; accepted 22 May 2024; published 11 June 2024)

Gramicidin A (gA) is a short hydrophobic β-helical peptide that forms cation-selective channels in lipid membranes in the course of transbilayer dimerization. The length of the gA helix is smaller than the thickness of a typical lipid monolayer. Consequently, elastic deformations of the membrane arise in the configurations of gA monomers, conducting dimer, and the intermediate state of coaxial pair, where gA monomers from opposing membrane monolayers are located one on top of the other. The gA channel is characterized by the average lifetime of the conducting state. The elastic properties of the membrane influence the average lifetime, thus making gA a convenient sensor of membrane elasticity. However, the utilization of gA to investigate the elastic properties of mixed membranes comprising two or more components frequently relies on the assumption of ideality, namely that the elastic parameters of mixed-lipid bilayers depend linearly on the concentrations of the components. Here, we developed a general approach that does not rely on the aforementioned assumption. Instead, we explicitly accounted for the possibility of inhomogeneous lateral distribution of all lipid components, as well as for membrane-mediated lateral interactions of gA monomers, dimer, coaxial pair, and minor lipid components. This approach enabled us to derive unknown elastic parameters of lipid monolayer from experimentally determined lifetimes of gA channel in mixed-lipid bilayers. A general algorithm was formulated that allows the unknown elastic parameters of a lipid monolayer to be obtained using gA as a mechanical sensor.

DOI: 10.1103/PhysRevE.109.064404

I. INTRODUCTION

Gramicidin A (gA) is a pentadecapeptide antibiotic produced by *Bacillus brevis*. In lipid membranes, gA forms a $\beta^{6.3}$ helix, the length of which is usually somewhat smaller than the thickness of one lipid monolayer [1–3]. Two gA monomers located in the opposing membrane leaflets can form a transmembrane dimer, which represents a cation-selective conducting channel [1–4]. The dimer is stabilized by up to six hydrogen bonds established between several *N*-terminal amino acids of two gA monomers [5]. The formation and dissociation of the channel are thought to occur via the state of a so-called coaxial pair, where two gA monomers are situated one on top of the other. The coaxial pair is assumed to correspond to the top of the energy barrier of the dimerization/dissociation processes [6–8]. Given that the length of the monomer is typically smaller than the thickness of a lipid monolayer, it can be inferred that gA induces elastic deformations of the membrane in its vicinity, regardless of whether the monomer is in a monomer state, a coaxial-pair state, or a conducting dimer state. The formation of the channel can be observed in electrophysiological experiments as an appearance of ionic current through the membrane [9–15]. The probability of channel formation and the average lifetime of the conducting state are strongly dependent on the elastic properties of the membrane [13–15]. This allows gA to be considered a deformation sensor in lipid membranes [16]. As observed experimentally [13–15] and obtained theoretically [6–8,17], the lifetime of the gA channel depends on the lipid composition of membranes, applied lateral tension, and the presence of membrane inclusions. The elastic deformations induced by gA have been the subject of analysis for decades [3,5,10–13,15,16,18–20]. However, as far as we are aware, previous works, commencing with the pioneering work by Huang [18], assumed that only dimer deforms the membrane, while deformations induced by gA monomers and coaxial pairs were ignored [12,15,16,18,21–24]. An exception is the work (Ref. [20]) which took into account the deformations induced by gA monomers when calculating the curvature stress using molecular dynamics (MD) simulations. In early models, the energy of the "gA dimer+membrane" system includes only the elastic energy of the deformed membrane [12,15,18,21,23]. The membrane is considered as an effective spring, the energy of which is proportional to the square of the difference between the length of gA dimer, l, and the bilayer thickness d_0 in the undeformed state (Hooke's law). However, with such reasoning, there is no energy barrier for the formation of a gA dimer from two gA monomers, since the energy of the system monotonically depends on the compression of the membrane $\sim (d_0-l)^2$, and therefore the energy is maximal in the dimer state. Later, elastic models were supplemented by taking into account inelastic energy contribution that stabilizes the dimer, for example, the energy of six hydrogen bonds that arise between two gA monomers during the formation of the dimer. It is assumed that the forces stabilizing the dimer act at a certain distance δ between the

*Contact author: academicoleg@yandex.ru
†Contact author: akimov_sergey@mail.ru

monomers, less than the difference $(d_0 - l)$ [16,22,24]. This leads to the fact that the maximum total energy of the system (the top of the energy barrier) is achieved somewhere between the states of the coaxial pair and the dimer (in our notation); the total energy in the coaxial-pair state is zero.

In Ref. [17], using the Mayer cluster expansion approach [25,26], it was shown that any membrane-deforming inclusions (for example, transmembrane or peripheral peptides) should change the lifetime of gA channels. The lifetime depends on the concentration of inclusions and how they deform the lipid bilayer. This approach can be directly applied to analyze the influence of lipid inclusions on the characteristics of gA channels. A membrane consisting of a mixture of lipids with one main component can be characterized as a single-component lipid membrane, the remaining lipid components of which are present in the form of lipid inclusions in a low concentration. This makes it possible to calculate the lifetime of gA channels in mixed-lipid membranes depending on the elastic parameters of the membranes and their concentration. It should be noted that this approach does not rely on the widely used (and sometimes erroneous [27]) assumption that elastic parameters of the lipid bilayer, such as spontaneous curvature, thickness, or inverse bending modulus, depend linearly on the concentration of lipid components. Our model takes into account the possibility of heterogeneous lateral distribution of all lipid components and their interaction with gA monomers, dimers, and coaxial pairs.

In this work, we have developed a method for applying the described approach to solve the inverse problem. We have demonstrated how unknown elastic parameters of lipid monolayer patches (minor components) can be obtained from experimentally determined lifetimes of the gA channel in mixed-lipid bilayers. We assumed that macroscopic elastic parameters can be attributed to a patch of the lipid monolayer, the area of which is equal to the area of a single lipid molecule. We used the experimental results obtained in Ref. [28]. In this work, the photoisomerizing lipid 3-hydroxypropane-1,2-diylbis(4-(4-((E)-(4-butylphenyl)diazenyl)phenyl)butanoate) (OptoDArG) was used. OptoDArG has an azobenzene *cis/trans* photoswitchable group in both hydrophobic tails. Another widely used photoswitchable lipid is 1-stearoyl-2-[(E)-4-(4-((4-butylphenyl) diazenyl)phenyl)butanoyl]-sn-glycerol (PhoDAG), which has an azobenzene group in only one tail. *Trans*-to-*cis* photoisomerization is induced by light at 365 nm; the opposite *cis*-to-*trans* photoswitching occurs upon irradiation with light at a wavelength of 430 nm. In the *trans* configuration, the tails of OptoDArG/PhoDAG are elongated and approximately straight, whereas in the *cis* configuration the tails are highly curved. The lifetime of gA channels was measured in lipid bilayers of the following composition: pure dioleoylphosphatidylcholine (DOPC); mixture of DOPC with 10 mol. % OptoDArG; pure diphytanoylphosphatidylcholine (DPhPC); and a mixture of DPhPC with 10 mol. % OptoDArG [28]. The dependence of the gA-channel lifetime on the concentration of admixture lipids 1,2-dioleoyl-sn-glycero-3-phosphoethanolamine (DOPE), PhoDAG, and OptoDArG was theoretically considered.

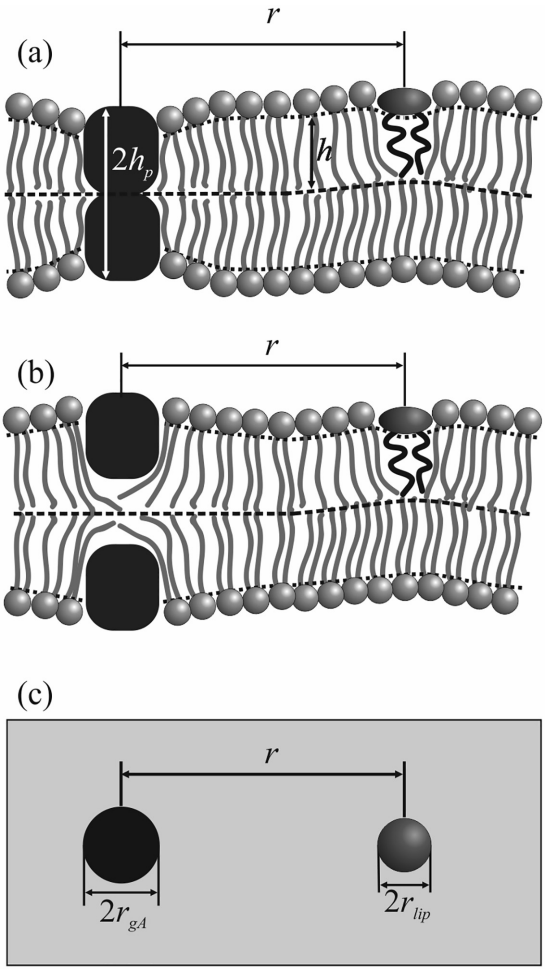

FIG. 1. Configurations that determine the lifetime of the gA dimer: (a) dimer; (b) coaxial pair; and (c) top view of the configurations (a) and (b). The lipidic inclusion is shown as the ellipse with two black tails [side view in (a), (b)] or as the circle with gradient filling [top view in (c)]. The monomer of gA is shown as the black rectangle [side view in (a), (b)] or as the black circle [top view in (c)].

II. METHODS

Consider a lipid membrane with embedded gA monomers and spontaneously formed transmembrane conductive dimers. The membrane contains an additional small amount of lipidic impurity—a lipid component that differs from the main lipid of the membrane, for example, DOPE, lysolipids, or photolipids such as PhoDAG and OptoDArG that are present in the membrane in a low concentration. In general, the lifetime of a gA dimer and the equilibrium concentration of dimers in the membrane are determined by the energies of three characteristic configurations of gA: a transmembrane dimer, a coaxial pair, and individual monomers (Fig. 1) [6]. It is assumed that the energy of up to six hydrogen bonds formed between several *N*-terminal amino acids of the two gA monomers forming a dimer is independent of the elastic properties of the membrane. Thus, the lifetime of the conducting state τ is determined by the difference in elastic energies of the configurations of the coaxial pair and the dimer. The

equilibrium concentration of dimers is determined by the difference of the energy of the dimer and the doubled energy of the monomer [6].

In all three configurations gA deforms the lipid membrane [3,5–8]. The energy of lipid bilayer deformations directly contributes to energies of gA configurations. For simplicity, we consider circular membrane inclusions, i.e., inclusions possessing a rotational symmetry with respect to some axis perpendicular to the membrane plane. When deformation-inducing objects, like gA or other membrane inclusions, are close to each other, the deformations overlap, leading to an effective lateral interaction of membrane inclusions. We denote $W(r)$ the energy of such interactions for a fixed distance r between the centers of two inclusions. Thus, membrane inclusions can be considered as a nonideal two-dimensional gas of particles, the interactions between which are mediated by deformations of the lipid membrane. Considering gA and a short transmembrane peptide WALP [29,30] as membrane-deforming inclusions, we recently have obtained [17] the dependences of the average lifetime and the equilibrium concentration of gA dimers in the membrane as a function of the gA and WALP concentrations, using Mayer's cluster expansion methods for a nonideal gas [25,26]. Briefly, Mayer's cluster expansion is the following. First, the partition function Z_0 of the membrane with embedded gA molecules and incorporated inclusions is derived in the zeroth approximation of ideal system with all interactions switched off. In Mayer's cluster expansion [25,26], the configuration partition function of a nonideal system is expressed as a product of specific functions of pairwise interaction potentials. These functions arise as a result of taking into account all possible positions of particles relative to the Gibbs weight of configurations. For gA monomers incorporated into two (upper and lower) leaflets of the membrane that are able to form conducting dimers, in the presence of inclusions, there are ten such pairwise interactions corresponding to the total number of ways to choose couples of particles from four types of particles present in the system: gA monomer in the upper monolayer (U), gA monomer in the lower monolayer (L), conducting dimer (D), inclusion (I): $U+U, U+L, L+L, U+D, L+D, U+I, L+I, D+D, I+I, D+I$. In the linear order of concentrations, only pairwise interactions should be taken into account. The higher-order corrections to the partition function can be obtained by means of correcting factors [25,26]. In particular, the second correction should include three-particle correlations yielding the factors in the partition function in an amount equal to the number of ways to select three particles from four types of particles (U, L, D, I) present in the membrane. Utilizing this approach, for known potential of pairwise interactions of the particles one can calculate the coordination partition function up to any desired order of concentrations [17]. The derived partition function allows calculating any average characteristics of the system. In particular, for a low-gA concentration, when corrections for the dimer-dimer interaction can be neglected, the average lifetime τ of the conducting dimer is given by [17]

$$\tau = \tau_0 \exp\Bigg[(\beta_{1,DI}-\beta_{1,PI})\frac{C_I}{1!}+(\beta_{1,DU}-\beta_{1,PU})\frac{C_U}{1!}+(\beta_{1,DL}-\beta_{1,PL})\frac{C_L}{1!}+(\beta_{2,DII}-\beta_{2,PII})\frac{C_I^2}{2!}$$
$$+(\beta_{2,DUU}-\beta_{2,PUU})\frac{C_U^2}{2!}+(\beta_{2,DLL}-\beta_{2,PLL})\frac{C_L^2}{2!}+(\beta_{2,DIU}-\beta_{2,PIU})\frac{C_IC_U}{1!1!}+(\beta_{2,DIL}-\beta_{2,PIL})\frac{C_IC_L}{1!1!}$$
$$+(\beta_{2,DUL}-\beta_{2,PUL})\frac{C_UC_L}{1!1!}+(\beta_{3,DIII}-\beta_{3,PIII})\frac{C_I^3}{3!}+\cdots\Bigg], \tag{1}$$

where τ_0 is gA dimer lifetime in the absence of membrane inclusions in the limit of zero gA monomer concentration; $\beta_{1,AB}=\int f_{AB}d\mathbf{r}_{AB}$ are the first Mayer's cluster integrals, corresponding to A–B particle interactions; A and B are particle types: dimers (D), coaxial pairs (P), monomers in upper (U) or lower (L) monolayers, membrane inclusion (I); $f_{AB}=e^{-(W_{AB}/k_BT)}-1$ is the Mayer function, W_{AB} is an interaction potential of particles A and B; k_B is the Boltzmann constant; T is the absolute temperature; C_A is the surface concentration of the particles A; $\beta_{2,ABC}=\frac{1}{S}\int\int\int f_{AB}f_{AC}f_{BC}d\mathbf{r}_A d\mathbf{r}_B d\mathbf{r}_C$ are the second Mayer's cluster integrals, corresponding to A–B–C particle interactions. The third Mayer's cluster integrals $\beta_{3,ABCD}$ are defined in a similar way. Further, we consider constant gA concentrations in both monolayers, so we can rewrite (1) as

$$\tau = \tau_0(C_U,C_L)\exp\Bigg[(\beta_{1,DI}-\beta_{1,PI})\frac{C_I}{1!}+(\beta_{2,DII}-\beta_{2,PII})\frac{C_I^2}{2!}+(\beta_{2,DIU}-\beta_{2,PIU})\frac{C_IC_U}{1!1!}+(\beta_{2,DIL}-\beta_{2,PIL})\frac{C_IC_L}{1!1!}$$
$$+(\beta_{3,DIII}-\beta_{3,PIII})\frac{C_I^3}{3!}+\cdots\Bigg]\approx\tau_0(C_U,C_L)\exp\left[(\beta_{1,DI}-\beta_{1,PI})C_I\right], \tag{2}$$

where $\tau_0(C_U,C_L)$ is the average lifetime of gA dimer in the membrane with fixed monomer concentrations in the upper- (C_U) and in the lower (C_L) monolayers without membrane inclusions. In the limit $C_U, C_L \to 0$, $\tau_0(C_U, C_L)\to\tau_0(0,0)=\tau_0$. The expression (2) can be generalized in an obvious way when there are several types of inclusions in the membrane: $\tau=\tau_0(C_U,C_L)\prod_i \exp[(\beta_{1,DI_i}-\beta_{1,PI_i})C_{I_i}]$, where the subscript index "i" enumerates the types of membrane inclusions.

On the right-hand side of Eq. (2) we neglected terms having the order of concentrations higher than the linear one. The neglected terms correspond to interactions of dimer or coaxial pair with clusters of monomers and membrane inclusions. Thus, in the low-concentration limit the average lifetime of gA

dimer is determined by the difference $(\beta_{1,DI} - \beta_{1,PI})$, where

$$\beta_{1,DI} = \int \left(\exp\left[-\frac{W_{DI}(r)}{k_B T} \right] - 1 \right) dS,$$
$$\beta_{1,PI} = \int \left(\exp\left[-\frac{W_{PI}(r)}{k_B T} \right] - 1 \right) dS, \quad (3)$$

and the integration is performed over all possible relative positions of two interacting particles.

In Ref. [17], we also calculated the average concentration of gA dimers as a function of the total surface concentration of gA (C_1 and C_2 in the upper- and lower monolayer, respectively) and concentration of membrane inclusions. In the case of low concentration of gA dimers, the dimer-dimer interactions can be neglected, and the dimer concentration is then given by

$$C_D = k_D C_U C_L, \quad C_D + C_U = C_1, \quad C_D + C_L = C_2, \quad (4)$$

where k_D is the so-called dimerization equilibrium constant. As it was shown in Refs. [7,17], generally k_D depends on concentrations of gA and membrane inclusions due to membrane-mediated interactions of the particles: $k_D = k_D(C_1, C_2, C_I)$. In the case of low concentrations, k_D can be expressed as follows:

$$k_D \approx k_{D0} \exp\left[(\beta_{1,DI} - \beta_{1,UI} - \beta_{1,LI}) C_I \right], \quad (5)$$

where k_{D0} is the value of k_D in the limit of zero concentration of membrane inclusions, i.e., $k_D \to k_{D0}$ when $C_I \to 0$. We should note that k_{D0} depends weakly on gA concentration [7] but it is independent of the concentration of membrane inclusions.

In Ref. [17], equations similar to (1)–([4]) were derived for the particular case of transmembrane inclusions. However, the derivation was quite general, and it could be applied for any membrane-deforming inclusions, e.g., lipidic inclusions such as liquid-ordered domains or rafts [31,32], as well as small lipidic patches [33]. Thus, one can expect that lipidic inclusion will interact with gA dimers and coaxial pairs through membrane deformations, and therefore they should alter the dimer lifetime and dimerization constant.

To determine the pairwise interaction energies $W_{AB}(r)$, we calculated the total energy of membrane deformations induced by two membrane-deforming particles located at fixed distances r from each other, and the energies of membrane deformations induced by single particle of each type. We obtain the energy of bilayer membrane deformations as a sum of elastic energies of two leaflets, using the functional of elastic deformations derived by Hamm and Kozlov in Ref. [34] and further developed in Refs. [6–8,17,33]:

$$\begin{aligned} W = & \int dS_u \left(\frac{B}{2} (\mathrm{div}\mathbf{n}_u + J_{0u})^2 - \frac{B}{2} J_{0u}^2 + \frac{K_t}{2} (\mathbf{n}_u - \mathbf{grad}\, H_u)^2 + \frac{\sigma_u}{2} (\mathbf{grad}\, H_u)^2 \right. \\ & \left. + \frac{K_a}{2h^2} \left(h - \frac{h^2}{2} \mathrm{div}\mathbf{n}_u + M - H_u \right)^2 + K_G K_u + \frac{K_{\mathrm{rot}}}{2} (\mathbf{rot}\, \mathbf{n}_u)^2 \right) \\ & + \int dS_l \left(\frac{B}{2} (\mathrm{div}\mathbf{n}_l + J_{0l})^2 - \frac{B}{2} J_{0l}^2 + \frac{K_t}{2} (\mathbf{n}_l + \mathbf{grad}\, H_l)^2 + \frac{\sigma_d}{2} (\mathbf{grad}\, H_l)^2 \right. \\ & \left. + \frac{K_a}{2h^2} \left(h - \frac{h^2}{2} \mathrm{div}\mathbf{n}_l - M + H_l \right)^2 + K_G K_l + \frac{K_{\mathrm{rot}}}{2} (\mathbf{rot}\, \mathbf{n}_l)^2 \right), \end{aligned} \quad (6)$$

where B is the splay modulus of lipid monolayer; $\mathbf{n}_u$ and $\mathbf{n}_l$ are unit vector fields on membrane surfaces (upper and lower, respectively) called directors, which characterize an average orientation of lipid tails; J_0 is the spontaneous curvature of lipid monolayer; K_t is the tilt modulus; σ is the lateral tension; H_u and H_l are z coordinates of the surfaces of the upper and lower monolayers; K_a is the stretching-compression modulus; h is the thickness of an unperturbed lipid monolayer; M is z coordinate of monolayer interface; K_G is the Gaussian modulus; K_{rot} is the twist modulus; the integration is performed over the surfaces of lipid monolayers; and the unperturbed membrane is assumed flat and parallel to Oxy plane with $M(x, y) = 0$, $H_{u,l}(x, y) = \pm h$. We assume that membrane deformations are small and use quadratic approximation for the elastic energy. We rewrite the director fields in the Cartesian coordinates as $\mathbf{n}_{l,u} = (n_x, n_y, \pm 1)$, where the both projections n_x and n_y are functions of coordinates x and y.

Different gA configurations (i.e., gA monomer, dimer, and coaxial pair) impose different boundary conditions on the functional (6). We denote the outline contour of gA at the surface of the lipid monolayer as Γ; thus, Γ is a circle of the fixed radius r_{gA} (Fig. 1). Following Refs. [6,7], we assume that gA dimer imposes the following boundary conditions at the contour Γ:

$$H_u(\Gamma) = H_0 + h_p$$
$$H_l(\Gamma) = H_0 - h_p, \quad (7)$$

where h_p is the length of the hydrophobic part of gA monomer, and H_0 is z coordinate of the dimer center of mass. H_0 is determined from a minimization of the functional (6). Boundary conditions imposed by gA monomer differ from (7):

$$n_{u,n}(\Gamma) = -\frac{h - h_p}{\sqrt{(h - h_p)^2 + h_p^2}},$$
$$n_{u,t}(\Gamma) = 0, \quad H_u(\Gamma) = H_m, \quad (8)$$

TABLE I. Parameters of lipid monolayers.

	B, k_BT [37,38]	K_t, mN/m [34]	K_a, mN/m [37]	K_{rot}, k_BT [35]	K_G, k_BT [35]	J_0, nm^{-1} [39]	h, nm [37]	r_{lip}, nm
DOPC	10	40	133	5	–5	−0.091	1.45	
DPhPC	14	40	133	7	–7	–0.097	1.4	
trans-PhoDAG	10	40	133	5	–5	−0.091	1.45	
trans-OptoDArG	10	40	133	5	–5	−0.091	1.45	
cis-PhoDAG	from 5 to 20	40	133	$B/2$	$-B/2$	from −0.6 to −0.1	1.45	0.472
cis-OptoDArG	from 5 to 20	40	133	$B/2$	$-B/2$	from −0.6 to 0	0.7	0.662
DOPE	10	40	133	$B/2$	$-B/2$	–0.35	1.45	0.472

where $n_{u,n}$ and $n_{u,t}$ are normal and tangential, respectively, components of the director (relative to the boundary contour Γ); H_m is z coordinate of the contour Γ; and H_m is determined from a minimization of the functional (6). The conditions (8) are written for gA monomer in the upper monolayer; for the lower one the conditions can be written in a similar way. Coaxial pair of gA imposes boundary conditions that are the combination of the conditions (8) that are imposed by both upper and lower gA monomers simultaneously. We neglected a possible tilt of gA dimer, monomer, or coaxial pair as a whole [17], because here we mainly focus on lipidic membrane inclusions that cause negligible tilt of gA species (data not shown).

Lipidic inclusions do not impose specific boundary conditions on the functional (6) except general conditions of the continuity of directors and monolayer surfaces. One just should use in (6) appropriate elastic moduli, spontaneous curvatures, and monolayer thickness for corresponding regions of the membrane. We assume that lipidic inclusion is a circle of the radius r_{lip}.

We add boundary conditions at infinity ($r = \infty$) based on that the deformations should decay far from the inducing objects:

$$\mathbf{n}_{l,u}(\infty) = (0, 0, \pm 1), \quad M(\infty) = 0,$$
$$H_u(\infty) = h, \quad H_l(\infty) = -h. \tag{9}$$

The minimization of the elastic energy functional (6) under the conditions (7)–(9) allows determining the energy of elastic deformations of the membrane. However, such a minimization cannot be completed analytically. We thus used the finite-element method with an adaptive mesh to minimize the functional (6) numerically. The minimization algorithm is described in detail in Refs. [8,35,36].

III. PARAMETERS OF THE SYSTEM

To obtain quantitative results, we used the values of the system parameters listed in Table I.

For *cis*-OptoDArG monolayer the bending modulus is unknown, so we considered it as a parameter varying in the range from $B = 5k_BT$ to $B = 20k_BT$ (per monolayer); the unknown spontaneous curvature of *cis*-OptoDArG was considered a parameter varying from $J_0 = -0.6\,nm^{-1}$ to $J_0 = 0$. For *cis*-PhoDAG monolayer the bending modulus is unknown, so we considered it as a parameter varying in the range from $B = 5k_BT$ to $B = 20k_BT$ (per monolayer); and the unknown spontaneous curvature of *cis*-PhoDAG was considered a parameter varying from $J_0 = -0.6\,nm^{-1}$ to $J_0 = 0$. For gA monomer: $r_{gA} = 1\,nm$ and $h_p = 0.75\,nm$ [6–8]. As the lifetimes of gA channel are similar in pure DOPC, pure DPhPC, and their mixtures with *trans*-OptoDArG [28], we assumed that the thickness h of *trans*-OptoDArG monolayer patch should be close to the thickness of DOPC, DPhPC monolayers, i.e., it should be about 1.4–1.45 nm. For the same reason, we made analogous assumption for other mechanical parameters of *trans*-OptoDArG monolayer. The thickness h of *cis*-OptoDArG monolayer patch was estimated based on its chemical structure; r_{lip} was then determined under the assumption of lipid volume conservation in the process of photoisomerization. Mechanical parameters of *trans*-PhoDAG monolayer were assumed to be the same as parameters of DOPC. The thickness h of *cis*-PhoDAG monolayer was assumed to be $h = 1.45\,nm$, which corresponds to that only one of two tails photoswitches.

In Ref. [6] it was shown that in a one-component lipid bilayer the average lifetime of gA channel τ_0 can be expressed as

$$\tau_0 = \frac{1}{\nu} V \exp\left[\frac{W_{pair} - W_{dimer}}{k_BT}\right], \tag{10}$$

where W_{pair} and W_{dimer} are the energies of membrane deformations induced by single gA coaxial pair and dimer, respectively, in an infinite lipid membrane with no other membrane-deforming objects; ν is a characteristic frequency of gA thermal motion that should be of the same order of magnitude for different lipids; V is the factor accounting for the energy contributions independent of membrane elastic properties, e.g., the energy of six hydrogen bonds stabilizing gA dimer. Using elastic parameters of DOPC and DPhPC monolayers, we estimated from (10) that gA lifetimes of 3.6 ± 1.1 and 4.5 ± 1.5 s determined in single-component DOPC and DPhPC membranes in Ref. [28], respectively, require the spontaneous curvature of DPhPC monolayer to be $J_{0DPhPC} = -0.097\,nm^{-1}$. This value differs from the $-0.2\,nm^{-1}$ obtained in Ref. [40]. Most probably, this difference is conditioned by the elevated temperature (35 C) and two-component lipid mixtures utilized in experiments of Ref. [40].

IV. RESULTS

Applying the formalism described above, we calculated the interaction energies of *cis*-OptoDArG with gA dimer

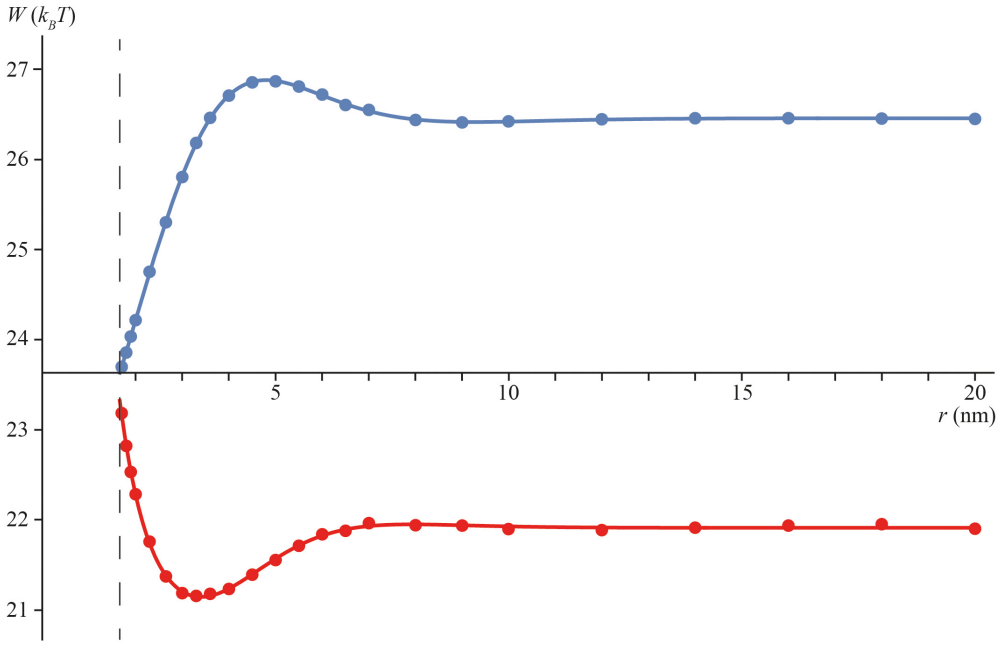

FIG. 2. The energy of deformations of DOPC membrane induced by gA dimer and *cis*-OptoDArG photolipid inclusion placed at a distance r from the dimer [blue (upper) line] or gA coaxial pair [red (lower) line]. These particular curves were calculated for monolayer bending modulus and spontaneous curvature of *cis*-OptoDArG $B = 10k_BT$, $J_0 = -0.2\,\mathrm{nm}^{-1}$. The points correspond to numerically calculated values at discreet r_i; the solid curves correspond to interpolated functions. The vertical dashed line denotes the smallest possible distance between gA dimer or coaxial pair and the lipidic inclusion.

and coaxial-pair configurations. As the bending modulus and spontaneous curvature of *cis*-OptoDArG and *cis*-PhoDAG monolayers are unknown, we performed the calculations for many pairs of B and J_0 taken from the ranges $5\,k_BT < B < 20\,k_BT$, $-0.6\,\mathrm{nm}^{-1} < J_0 < 0$. Figure 2 illustrates the total energies of deformations induced by gA dimer and lipidic inclusion and by gA coaxial pair and lipidic inclusion in the particular case of lipidic inclusion parameters $B = 10k_BT$ (per monolayer), $J_0 = -0.2\,\mathrm{nm}^{-1}$. The calculations were performed for a discrete set of distances r between gA and lipidic inclusion centers [Fig. 1(c)]: $r_i = 1.7$, 1.8, 1.9, 2.0, 2.3, 2.65, 3.0, 3.3, 3.65, 4.0, 4.5, 5.0, 5.5, 6.0, 6.5, 7.0, 8.0, 9.0, 10.0, 12.0, 14.0, 16.0, 18.0, and 20.0 nm. For the subsequent integration aimed at calculating Mayer's cluster integrals, the obtained discrete values of the elastic energy were interpolated by the function having the form $W_0 + P_6(r) \times \exp(-qr)$, where W_0 is a constant equal to the sum of the elastic energies induced by solitary gA coaxial pair or gA dimer and lipidic inclusion, $P_6(r)$ is a polynomial of the sixth order, and q is an inverse length of the interaction decay. From this definition, we get the interaction energies $W_{PI}(r)$ and $W_{DI}(r)$ in the approximate form $W_{AB}(r) = P_6(r) \times \exp(-qr)$. We assumed that Mayer's integrals (3) are mainly accumulated in the vicinity of gA dimer or coaxial pair, i.e., at small r, so we do not need to know the exact details of interactions at large distances, where the interaction energies are exponentially small [33], although there the error arising from numeric calculations is multiplied by a relatively large factor $2\pi r$. From Fig. 2 it is seen that the interpolation function is close to the numerically calculated values and describes them adequately. In the case of *cis*-PhoDAG there is no thickness mismatch with the surrounding lipid, and the interaction energies are approximately one order of magnitude smaller (data not shown). Especially, in the case when J_0 is close to $J_{0\mathrm{DOPC}}$ the interaction energies are so small, that numerical error arising from discrete and finite mesh in the finite-element method becomes important. To suppress the influence of such errors we integrated $\beta_{1,DI}$ and $\beta_{1,PI}$ in (3) not from $r = 0$ to $+\infty$, but from $r = 0$ to $r_{\max}$, where $r_{\max}$ corresponds to zeros of $W_{DI}(r)$ and $W_{PI}(r)$; $r_{\max}$ is approximately 5–7 nm.

We calculated Mayer's cluster integrals $\beta_{1,DI}$ and $\beta_{1,PI}$ for gA in DOPC considering DOPE as a lipidic impurity. We obtained the values $\beta_{1,DI} = -8.85\,\mathrm{nm}^2$ and $\beta_{1,PI} = 4.25\,\mathrm{nm}^2$. To check the applicability of the expansion to first order on concentrations, we also calculated Mayer's cluster integrals $\beta_{2,DII}$ and $\beta_{2,PII}$ in cases of gA dimer and coaxial pair interacting with two DOPE lipidic inclusions in the same monolayer and in opposite monolayers. In Fig. 3 the dependence of τ/τ_0 on surface concentration of DOPE inclusions is shown. The dependence is obtained using Eq. (2). It is clear from Fig. 3 that the corrections of higher than the linear order in (2) can be neglected for the DOPC + DOPE mixture. We assume that this statement will be true in case of any inclusions, which relatively weakly deform the membrane.

We calculated Mayer's cluster integrals $\beta_{1,DI}$ and $\beta_{1,PI}$ for *cis*-OptoDArG in DOPC and DPhPC membranes, varying *cis*-OptoDArG splay modulus (per monolayer) in the range $5\,k_BT < B < 20\,k_BT$ and spontaneous curvature—in the range $-0.6\,\mathrm{nm}^{-1} < J_0 < 0$. The differences $(\beta_{1,DI} - \beta_{1,PI})$ are shown for DOPC [Fig. 4(a)] and DPhPC [Fig. 4(b)] membranes. The solid blue and red lines in Fig. 4 correspond to experimental results from Ref. [28], recalculated from the measured lifetimes according to Eq. (2) under the assumption of applicability of the first order on concentration expansion.

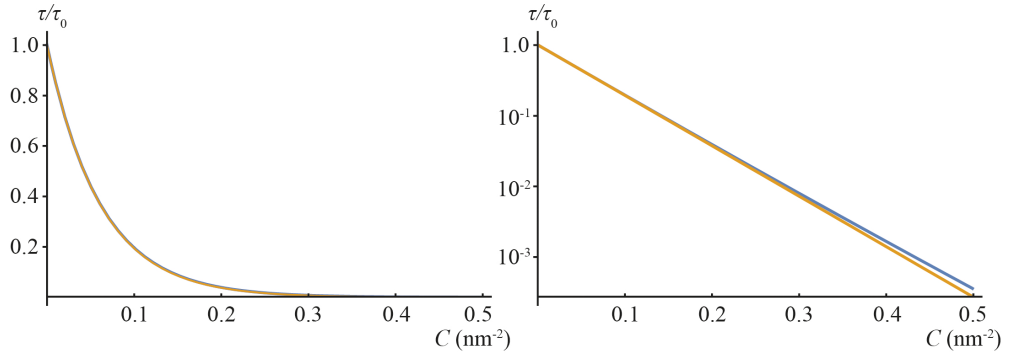

FIG. 3. The lifetime of single gA channel as the function of total surface concentration $C = C_1 + C_2$ of DOPE lipidic inclusion, where C_1, C_2 are the surface concentrations of DOPE lipidic inclusion per monolayer. The curves correspond to series expansion Eq. (2) up to first [blue (upper) line] and second [orange (lower) line] order of concentrations. The dependencies are shown in linear (a) and logarithmic (b) scales.

As the interaction potentials of *cis*-OptoDArG and gA dimer and coaxial-pair configurations are quite strong (see Fig. 2; the interaction energies are greater than k_BT), it is necessary to check whether we can neglect higher-order corrections of concentrations in Eq. (2). We calculated integrals $\beta_{2,DII}$ and $\beta_{2,PII}$ for several (B, J_0) points (data not shown) and found that for 10 mol. % concentrations of *cis*-OptoDArG, the higher-order corrections cannot be neglected: the common order of magnitude of $(\beta_{2,DII} - \beta_{2,PII})$ is $10^3\,\mathrm{nm}^4$. For such strongly interacting inclusions the linear theory can still be applied, but for very small concentrations only $C << (\beta_{1,DI}\text{-}\beta_{1,PI})/(\beta_{2,DII}\text{-}\beta_{2,PII})$; this value is much less than 1 mol. %. We expected that the intersection of the blue and red curves in Fig. 4 would allow us to determine exactly the *cis*-OptoDArG monolayer splay modulus and spontaneous curvature. However, within the experimental error of the gA lifetime measurements in Ref. [28] of approximately of 1/3 of the measured lifetime values, we found that the red and blue curves from Fig. 4 actually represent rather wide bands that overlap in wide ranges of B and J_0 (Fig. 5). The region of overlapping blue and red bands in Fig. 5 determines the possible range of elastic parameters of *cis*-OptoDArG monolayer. From Fig. 5 it follows that B and J_0 cannot be accurately determined simultaneously based on the experimental data of Ref. [28]. However, for reasonable values of the bending modulus $7\,k_BT < B < 15\,k_BT$, the spontaneous curvature of *cis*-OptoDArG monolayer can be confined to the range of $-0.49 < J_0 < -0.33\,\mathrm{nm}^{-1}$.

We calculated Mayer's cluster integrals $\beta_{1,DI}$ and $\beta_{1,PI}$ for *cis*-PhoDAG in DOPC and DPhPC membranes, varying *cis*-PhoDAG monolayer splay modulus (per monolayer) in the range $5\,k_BT < B < 20\,k_BT$ and spontaneous curvature in the range $-0.6\,\mathrm{nm}^{-1} < J_0 < -0.1\,\mathrm{nm}^{-1}$. The differences $(\beta_{1,DI} - \beta_{1,PI})$ are shown for DOPC [Fig. 6(a)] and DPhPC [Fig. 6(b)] membranes.

V. DISCUSSION

In the present work we developed a formalism that allows predicting the average lifetime of gA channels in lipid membranes with incorporated lipidic inclusions. Within the formalism, gA can be used as a sensor of mechanical

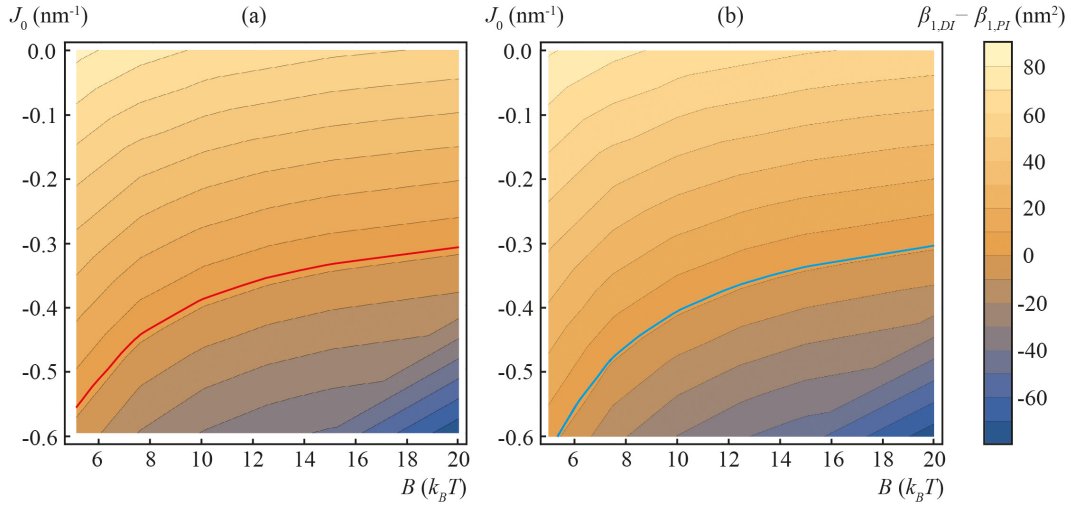

FIG. 4. The differences $(\beta_{1,DI} - \beta_{1,PI})$ calculated for different values of *cis*-OptoDArG monolayer bending modulus and spontaneous curvature in DOPC (a) and DPhPC (b) membranes. The red [panel (a)] and blue [panel (b)] curves correspond to experimental values of gA dimer lifetime determined in Ref. [28], recalculated to Mayer cluster integrals $(\beta_{1,DI} - \beta_{1,PI})$ using Eq. (2).

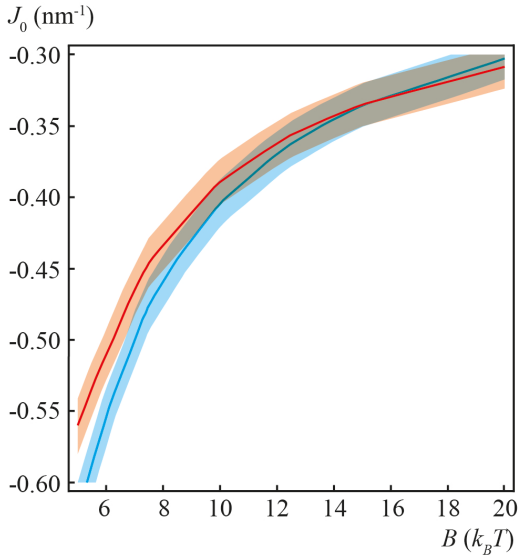

FIG. 5. Possible values of spontaneous curvature J_0 and splay modulus B of *cis*-OptoDArG monolayer calculated from the experimental data of Ref. [28] accounting for the experimental error of the gA lifetime measurements. Red (upper) and blue (lower) bands correspond to experiments performed on DOPC and DPhPC membranes, respectively; red (upper) and blue (lower) lines are taken from Fig. 4.

deformations of nonhomogeneous lipid membranes, containing laterally interacting lipidic impurities in a low concentration. This approach is based on statistical mechanics methods (like Mayer's cluster expansion) and takes into account the lateral redistribution of inclusions in the vicinity of gA. Recently, a similar approach was applied to explain an anomalous dependence of the current relaxation time of channels formed from gA analogs with *N*-terminal valine replaced by glycine ([Gly1]gA) or tyrosine ([Tyr1]gA) on their surface concentrations [7]. For these analogs, the inverse relaxation time decreased with increasing surface concentration of gramicidin, while for gA the dependence was monotonically increasing. Within the classic consideration of gramicidin in a membrane as an ideal gas of non-interacting particles [41], the anomalous dependence led immediately to the conclusion that the dimerization constant for gramicidin analogs should be negative. However, this contradiction is resolved within a generalized model that takes into account lateral interactions of gramicidin species mediated by membrane deformations. The model is analogous to the presented here; it is also based on the statistical approach allowing calculating the partition function of the system of interacting particles via Mayer's cluster expansion. The results of Ref. [7] thus validate to some extent the statistical approach utilized here.

For our calculations, we did not use the assumption that elastic parameters of a mixed-lipid bilayer depend linearly (or somehow else) on elastic parameters of monolayers of its constituent individual components. The elastic parameters calculated in the linear approximation within our statistical model appeared to differ considerably from those obtained using the ideal approximation of weighted average parameters [28]. For example, we estimated the spontaneous curvature of *cis*-OptoDArG monolayer to lie in the range from -0.49 to $-0.33\,\mathrm{nm}^{-1}$ (for the values of the bending modulus of *cis*-OptoDArG monolayer $7\,k_BT < B < 15\,k_BT$, which seems quite likely); this range is very far from the value $J_0 = -1.1\,\mathrm{nm}^{-1}$ obtained in the framework of the ideal model [28]. The results of our work imply that the conclusions following from the ideal model should be reconsidered in a more rigorous way, not only in the case of gA channels in multicomponent membranes, but also in more general cases, e.g., determination of lipid elastic parameters from experiments on lipid mixtures.

From our consideration it follows that membrane-deforming inclusions can be conventionally divided to strongly and weakly interacting with gA monomers, dimers, and coaxial pairs. For weakly interacting inclusions the linear approximation is valid until relatively large concentrations of the inclusions. The critical concentration of switching from the linear to nonlinear regime is determined by the condition that in the series over concentrations, Eq. (1), the second-order terms become comparable with the first-order terms, i.e.,

$$C \sim \frac{\beta_{1,AB} - \beta_{1,CD}}{\beta_{2,ABC} - \beta_{2,DEF}}, \tag{11}$$

where $\beta_{1,AB}$, $\beta_{1,CD}$, $\beta_{2,ABC}$, and $\beta_{2,DEF}$ are corresponding Mayer's integrals. Membrane inclusions that slightly alter monolayer or bilayer thickness, or just induce spontaneous curvature (like *trans*-OptoDArG, PhoDAG, DOPE, etc.), are generally weakly interacting. Inclusions that substantially alter the thickness of lipid monolayer or bilayer are generally strongly interacting. For example, for *cis*-OptoDArG the upper-limit concentration of the linear regime is less than 1 mol. %. In Ref. [28] the concentration of OptoDArG in the model membrane was 10 mol. % and thus our developed linear formalism that allows determining elastic parameters of lipidic inclusions is not directly applicable: higher-order terms should be taken into account in the series of gA-channel lifetime over concentration, Eq. (1). Physically, this implies that strongly interacting inclusions are attracted to gA dimers and even at a low concentration they form clusters comprising so many molecules that the inclusion-inclusion interaction inside the cluster cannot be neglected. Thus, the data on *cis*-OptoDArG monolayer splay modulus and spontaneous curvature, illustrated in Figs. 4 and 5, cannot be considered valid, as they were obtained in the linear approximation that is not applicable for the case of OptoDArG concentration of 10 mol. %. Thus, the derivation of *cis*-OptoDArG monolayer elastic parameters should be considered as an illustration of the method only. From our estimates it follows that for *cis*-OptoDArG the linear regime is violated at concentrations less than 1 mol. %. This means that for this lipid the widely used approximation of ideal mixture of noninteracting particles that lead to elastic parameters of the mixture being weighted average of elastic parameters of particular components almost never works. At the same time, the linear approximation is predicted to work quite well for weakly interacting inclusions like PhoDAG or DOPE (Fig. 3). The validity of the predictions can be checked experimentally. However, the experiments should be done on solvent-free model membranes, containing a lipidic impurity in a low concentration. At the moment,

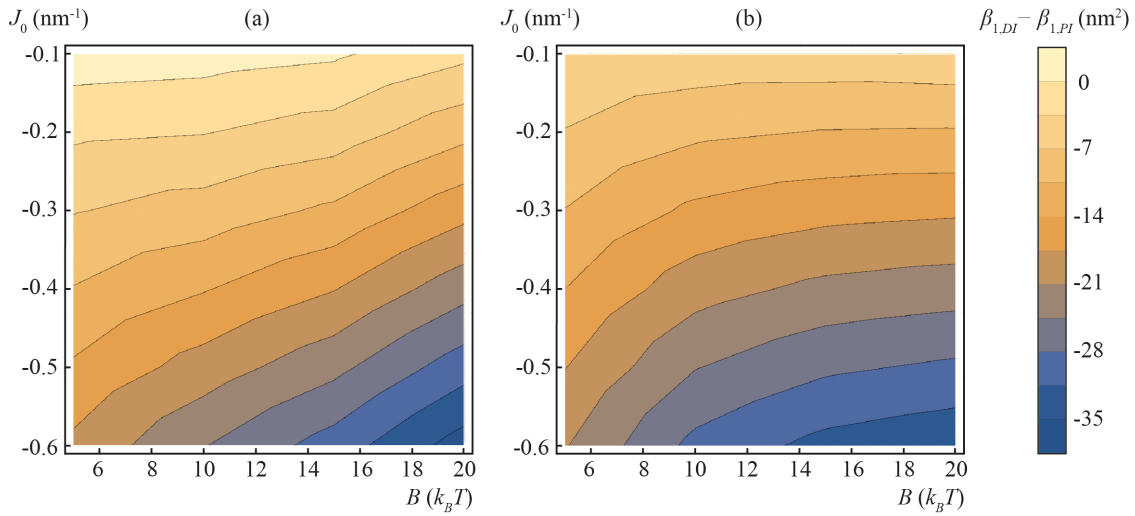

FIG. 6. The differences ($\beta_{1,DI} - \beta_{1,PI}$) calculated for different values of *cis*-PhoDAG monolayer splay modulus and spontaneous curvature in DOPC (a) and DPhPC (b) membranes.

as far as we know, there are no such experimental works: most experiments are performed on membranes formed using decane or other organic solvent [9,12,13,15,19,42], and the concentration of lipidic impurities is usually of the order of ten to tens molar percent [15,19,28].

Local enrichment/depletion of different lipid species in the vicinity of gA dimer was observed by means of MD in Refs. [19,20]. The membrane was formed from either single "reference" lipid or binary 1:1 mixture of lipids with the length shorter and longer than the length of the reference lipid. A local enrichment of shorter lipid (and depletion of longer lipid) was observed in the vicinity of gA dimer. The enrichment of the shortest lipid (shorter than the reference lipid by four CH_2 groups) achieved about 20 mol. % [19]. The average lifetime of gA channel was experimentally determined in model membranes of the same lipid composition as that used in MD. Qualitatively, the lifetime increased in binary lipid mixtures, as the dimer can recruit shorter lipids to its immediate neighborhood, thus partially relaxing the elastic stress that arises from the mismatch between the average membrane thickness and the length of the gA dimer. The elastic stress was estimated in the framework of simple elastic model, developed earlier and utilized in many works [16,19,21,24]. In the case of almost zero spontaneous curvature of the lipid monolayer, the model accounts for deformational mode of compression–stretching only, considering lipid monolayer as an effective spring. The equilibrium monolayer thickness (or equilibrium length of the effective spring) was taken from MD data. The experiments on the measurement of gA-channel lifetime were performed on model membranes containing decane as a solvent; the equilibrium thickness of such membranes is about 1 nm larger than the thickness of solvent-free membranes of the same lipid composition [19]. Nevertheless, the monolayer thickness for calculations was taken from MD data, i.e., from the solvent-free system. The reasoning for this choice was that gA dimer compresses the membrane, and thus in the vicinity of the dimer the solvent should be expelled from the space between two lipid leaflets, providing locally the bilayer equilibrium thickness as in a solvent-free membrane. Despite the apparent logic of such reasoning, the conclusions contradict experimental data. In decane-based membrane formed from dioleoylphosphatidylcholine (DOPC) the average lifetime of gA channel is about 0.53 s [19], while in the solvent-free DOPC membrane the lifetime of about 3.6 s was measured [28], i.e., an order of magnitude higher. In addition, simple elastic models developed and utilized in Refs. [19,20] for the analysis of lateral redistribution of lipids around gA dimer do not take into account the entropic contribution to the free energy of the system, although such contribution can be substantial, and it is automatically taken into account in MD.

In order to determine the average properties [e.g., channel lifetime, Eq. (2)] of a mixed system with membrane-mediated interactions, one should construct the partition function of the system. Such approach accounts automatically for the entropic contributions to the free energy of the system. The averaging over all possible configurations of membrane-deforming inclusions yields the corresponding exponential factors in Eqs. (1), (2), and (5). Here, the partition function was obtained via Mayer's cluster expansion, the cluster integrals of which [Eq. (3)] exploit the pairwise interaction potentials that are mediated by membrane deformations. The calculation of lateral distributions of deformations and their energy strongly relies on boundary conditions [Eqs. (7)–(9)] imposed by membrane-deforming inclusions. The particular type of the boundary conditions imposed by gramicidin is a matter of debate [18,20,21,23], starting from the pioneering work by Huang [18]. In most works, gA monomer does not impose any boundary conditions, as it is usually thought to induce no deformations. The exceptions are Refs. [6–8,17,20], where the deformations arising around gA monomers were explicitly taken into account. Dimer imposes the condition of fixed bilayer thickness [6–8,17–19,22–24]. Several works analyzed the effect of the condition imposed on the contact angle (slope) of lipid monolayer surface at the gA dimer boundary [18,21,23,24]. Generally, two cases are considered: zero contact angle and free (unrestrained) contact angle; the latter case was recently shown to better correspond to the data

obtained from MD modeling and experiments [20]. However, the boundary condition of fixed contact angle seems unphysical, as there are no physical forces that gA can impose on the contact angle of the monolayer surface, i.e., on the derivative of its shape. The gA dimer can only impose an appropriate orientation on its immediately adjacent lipids [i.e., fix the boundary director, e.g., according to Eq. (8)], but it cannot arrange several shells of the surrounding lipids to restrain the derivative of the monolayer surface, as there are no long-range physical forces in the system that could ensure this arrangement. At the same time, in elastic models that do not consider tilt deformation, setting the boundary director is equivalent to fixing the contact angle of the monolayer surface, as in the absence of tilt, director and unit normal to the surface do coincide. In this case the slope of the monolayer surface at gA dimer boundary reflects the actual shape of gA dimer. In some works the shape is assumed cylindrical [18]. In the absence of tilt, this assumption should result in the conditions of zero slope of the monolayer surface at gA dimer boundary. Allowing a nonzero slope silently means that the actual shape of gA dimer is assumed not cylindrical, but hourglass-like (negative slope) or barrel-like (positive slope). Consequently, the shape of gA monomer in these cases should be conical. Along with mismatch between gA length and lipid monolayer thickness, noncylindrical gA monomer should induce deformations of the membrane. Thus, theoretical models that simultaneously: (1) consider a mismatch between the length of gA dimer and membrane thickness; (2) do not fix zero slope of the monolayer surface at gA dimer boundary (i.e., that implies that the dimer shape is not cylindrical); (3) do not account explicitly for the tilt deformation; and (4) ignore deformations induced by gA monomers, are self-contradictory. The conclusions of the models that do fix zero slope of the monolayer surface, though, do not agree with the data of MD [20]. This contradiction can be resolved by accounting for deformations induced by gA monomers and considering the deformational mode of tilt.

Tilt is associated with an energy penalty. However, tilt modulus K_t is several times smaller than the stretching–compression modulus K_a (see Table I). This means that if the lateral stretching–compression is taken into account, tilt deformation should be accounted for with all the more reason. The stretching–compression deformation is formally used to compensate for the mismatch between the thickness of lipid bilayer and the length of gA dimer [18,21,24]. However, the thickness mismatch can be compensated for by any pair of deformations: splay, tilt, and stretching–compression [43,44]. Many works on energetics of gA-induced bilayer deformations utilize the pair of splay and stretching–compression [18,20,21,23]. But, tilt modulus K_t is several times smaller than the stretching–compression modulus K_a (see Table I), and thus it is more reasonable to utilize the pair of splay and tilt to compensate for the thickness mismatch. The significance of tilt was demonstrated in Ref. [20], where lipid directors were shown to deviate from normal to the monolayer surface, especially in the vicinity of gA dimer. If tilt deformation is considered, the shape of the monolayer surface no longer uniquely determines the state or energy of the system, as tilt provides an additional degree of freedom: lipids can be arbitrarily tilted with respect to the monolayer surface of a fixed shape. For this reason, even if the shape of the monolayer surface were obtained from all-atom MD, the calculated energy of the membrane would be model dependent [20].

Splay deformation can locally alter the monolayer thickness if the monolayer considered locally volumetrically incompressible [34], i.e., the volume of any element of monolayer does not change upon deformations. Under such condition, the splay deformation transforming rectangular elements of lipid monolayer to trapezium-like of equal volume should be accompanied by change in monolayer thickness [34]. The condition of volumetric incompressibility is used in many studies of elastic deformation induced by gA dimers. However, as a rule, this condition is utilized quite selectively: it is applied for the deformation of lateral stretching–compression, thus transforming it to the deformation of decrease–increase, respectively, of monolayer thickness [20,21,24]. The influence of the splay deformation on the monolayer thickness via volumetric incompressibility is usually ignored.

In several works the splay deformation arising in the vicinity of gA dimer was taken into account to some extent: such consideration was aimed at describing experiments on the dependence of gA-channel characteristics on spontaneous curvature of membrane leaflets [15,16]. As far as we know, the rigorous elastic-energy functionals like Eq. (6) were not used for the descriptions. Instead, a formal series of the elastic energy taken over the thickness mismatch $(d_0 - l)$ and monolayer spontaneous curvature c_0 is utilized: $\Delta G_{\rm def} = H_B(l-d_0)^2 + H_X(l-d_0)c_0 - H_C\, c_0^2$ [15,16]. However, such series is not exactly correct if gA dimer sets any nonzero boundary director. Indeed, the term proportional to $\sim \mathrm{div}(\mathbf{n})c_0$ in the elastic-energy functional like Eq. (6) can be explicitly integrated, leading to the term proportional to $\sim c_0 n_0$ (n_0 is the projection of the boundary director onto the membrane plane) that is linear on c_0, but does not include the thickness mismatch factor $(l - d_0)$. Such a term should stand in expression for the elastic energy in models that do not explicitly set the zero slope of the monolayer surface at the gA dimer boundary, i.e., in the most elastic models of membrane deformations induced by gA dimer.

In general, our approach allows determining unknown elastic parameters of lipid monolayers from experimentally measured lifetimes of gA channels. One should perform such measurements on solvent-free membranes composed of binary mixtures of known lipid with unknown lipid; the number of such binary mixtures (i.e., the number of utilized known lipids) should be equal to the number of elastic parameters of the unknown lipid monolayer one wants to determine. [The deformations induced in the membrane by the unknown lipid should be small; mainly, the thickness mismatch should be small to ensure the validity of the linear approximation according to Eq. (2).] The results of each experiment will determine the manifold in the space of elastic parameters (e.g., the line in two-dimensional $B - J_0$ space in our particular case, Fig. 4), and the intersections of the manifolds obtained in different experiments will determine the possible values of the needed parameters. The spontaneous curvature J_0 is always multiplied by the splay modulus B, and thus J_0 cannot be determined independently of B. However, there

is a term $\sim B\mathrm{div}(\mathbf{n})^2$ in the functional of elastic energy (6) that includes B but is independent of J_0. Thus, B and J_0 can both be determined for the investigated lipid inclusion if gA-channel lifetime is measured in two types of membranes, each formed from binary mixture of some matrix lipid and the investigated lipid inclusions; the elastic parameters of matrix lipid monolayers of two binary mixtures should be substantially different. Of note, the gA lifetimes should be determined quite precisely; otherwise, instead of a single point determined from the manifold intersections, one will obtain a multidimensional range of possible values of the unknown parameters. Practically, it is preferable to use membranes formed from known lipids having substantially different elastic parameters. In our case, DOPC and DPhPC bilayers are quite similar from the point of view of elasticity; this resulted in quite similar level-line behavior leading to a small intersection angle of blue and red curves in Figs. 4 and 5, thus yielding a relatively wide range of possible values of B, J_0 of *cis*-OptoDArG monolayer. It seems reasonable that if the experimental data of gA lifetimes were obtained on membranes characterized by substantially different elastic parameters, the curves would intersect at a large angle that might increase the accuracy of B, J_0 determination. The bending modulus of the matrix lipid can be experimentally varied in a wide range: from $6.8\,k_BT$ (dimyristoylphosphatidylcholine) [37] to $14\,k_BT$ (DPhPC) [38], thus potentially making it possible to utilize the developed approach.

ACKNOWLEDGMENT

This work was supported by the Russian Science Foundation (Grant No. 22-13-00435).

[1] E. Bamberg, H. J. Apell, and H. Alpes, Structure of the gramicidin A channel: Discrimination between the πL, D and the β helix by electrical measurements with lipid bilayer membranes, Proc. Natl. Acad. Sci. USA **74**, 2402 (1977).

[2] A. S. Arseniev, I. L. Barsukov, V. F. Bystrov, A. L. Lomize, and Y. A. Ovchinnikov, 1H-NMR study of gramicidin A transmembrane ion channel: Head-to-head right-handed, single-stranded helices, FEBS Lett. **186**, 168 (1985).

[3] T. Kim, K. I. Lee, P. Morris, R. W. Pastor, O. S. Andersen, and W. Im, Influence of hydrophobic mismatch on structures and dynamics of gramicidin A and lipid bilayers, Biophys. J. **102**, 1551 (2012).

[4] S. B. Hladky and D. A. Haydon, Ion transfer across lipid membranes in the presence of gramicidin A: I. Studies of the unit conductance channel, Biochim. Biophys. Acta **274**, 294 (1972).

[5] D. Sun, S. He, W. D. Bennett, C. L. Bilodeau, O. S. Andersen, F. C. Lightstone, and H. I. Ingólfsson, Atomistic characterization of gramicidin channel formation, J. Chem. Theor. Comput. **17**, 7 (2020).

[6] O. V. Kondrashov, T. R. Galimzyanov, K. V. Pavlov, E. A. Kotova, Y. N. Antonenko, and S. A. Akimov, Membrane elastic deformations modulate gramicidin A transbilayer dimerization and lateral clustering, Biophys. J. **115**, 478 (2018).

[7] O. V. Kondrashov, T. I. Rokitskaya, O. V. Batishchev, E. A. Kotova, Y. N. Antonenko, and S. A. Akimov, Peptide-induced membrane elastic deformations decelerate gramicidin dimer-monomer equilibration, Biophys. J. **120**, 5309 (2021).

[8] O. V. Kondrashov, T. R. Galimzyanov, R. J. Molotkovsky, O. V. Batishchev, and S. A. Akimov, Membrane-mediated lateral interactions regulate the lifetime of gramicidin channels, Membranes **10**, 368 (2020).

[9] A. M. O'Connell, R. E. Koeppe, and O. S. Andersen, Kinetics of gramicidin channel formation in lipid bilayers: Transmembrane monomer association, Science **250**, 1256 (1990).

[10] T. L. Jones, R. Fu, F. Nielson, T. A. Cross, and D. D. Busath, Gramicidin channels are internally gated, Biophys. J. **98**, 1486 (2010).

[11] T. I. Rokitskaya, Y. N. Antonenko, and E. A. Kotova, Photodynamic inactivation of gramicidin channels: A flash-photolysis study, Biochim. Biophys. Acta **1275**, 221 (1996).

[12] J. A. Lundbaek and O. S. Andersen, Lysophospholipids modulate channel function by altering the mechanical properties of lipid bilayers, J. Gen. Physiol. **104**, 645 (1994).

[13] J. A. Lundbæk, A. M. Maer, and O. S. Andersen, Lipid bilayer electrostatic energy, curvature stress, and assembly of gramicidin channels, Biochemistry **36**, 5695 (1997).

[14] J. R. Elliott, D. Needham, J. P. Dilger, and D. A. Haydon, The effects of bilayer thickness and tension on gramicidin single-channel lifetime, Biochim. Biophys. Acta **735**, 95 (1983).

[15] A. M. Maer, R. Rusinova, L. L. Providence, H. I. Ingólfsson, S. A. Collingwood, J. A. Lundbæk, and O. S. Andersen, Regulation of gramicidin channel function solely by changes in lipid intrinsic curvature, Front. Physiol. **13**, 836789 (2022).

[16] J. A. Lundbæk, S. A. Collingwood, H. I. Ingólfsson, R. Kapoor, and O. S. Andersen, Lipid bilayer regulation of membrane protein function: Gramicidin channels as molecular force probes, J. R. Soc. Interface **7**, 373 (2010).

[17] O. V. Kondrashov and S. A. Akimov, Regulation of antimicrobial peptide activity via tuning deformation fields by membrane-deforming inclusions, Int. J. Mol. Sci. **23**, 326 (2022).

[18] H. W. Huang, Deformation free energy of bilayer membrane and its effect on gramicidin channel lifetime, Biophys. J. **50**, 1061 (1986).

[19] A. H. Beaven, A. M. Maer, A. J. Sodt, H. Rui, R. W. Pastor, O. S. Andersen, and W. Im, Gramicidin A channel formation induces local lipid redistribution I: Experiment and simulation, Biophys. J. **112**, 1185 (2017).

[20] A. J. Sodt, A. H. Beaven, O. S. Andersen, W. Im, and R. W. Pastor, Gramicidin A channel formation induces local lipid redistribution II: A 3D continuum elastic model, Biophys. J. **112**, 1198 (2017).

[21] C. Nielsen, M. Goulian, and O. S. Andersen, Energetics of inclusion-induced bilayer deformations, Biophys. J. **74**, 1966 (1998).

[22] J. A. Lundbæk and O. S. Andersen, Spring constants for channel-induced lipid bilayer deformations estimates using gramicidin channels, Biophys. J. **76**, 889 (1999).

[23] C. Nielsen and O. S. Andersen, Inclusion-induced bilayer deformations: Effects of monolayer equilibrium curvature, Biophys. J. **79**, 2583 (2000).

[24] M. Goulian, O. N. Mesquita, D. K. Fygenson, C. Nielsen, O. S. Andersen, and A. Libchaber, Gramicidin channel kinetics under tension, Biophys. J. **74**, 328 (1998).

[25] J. E. Mayer and E. Montroll, Molecular distribution, J. Chem. Phys. **9**, 2 (1941).

[26] N. G. Van Kampen, A simplified cluster expansion for the classical real gas, Physica **27**, 783 (1961).

[27] A. J. Sodt, R. M. Venable, E. Lyman, and R. W. Pastor, Nonadditive compositional curvature energetics of lipid bilayers, Phys. Rev. Lett. **117**, 138104 (2016).

[28] J. Pfeffermann, B. Eicher, D. Boytsov, C. Hannesschlaeger, T. R. Galimzyanov, T. N. Glasnov, G. Pabst, S. A. Akimov, and P. Pohl, Photoswitching of model ion channels in lipid bilayers, J. Photochem. Photobiol. B **224**, 112320 (2021).

[29] M. B. Ulmschneider and J. P. Ulmschneider, Membrane adsorption, folding, insertion and translocation of synthetic trans-membrane peptides, Mol. Membr. Biol. **25**, 245 (2008).

[30] T. Bereau, W. D. Bennett, J. Pfaendtner, M. Deserno, and M. Karttunen, Folding and insertion thermodynamics of the transmembrane WALP peptide, J. Chem. Phys. **143**, 243127 (2015).

[31] L. J. Pike, Rafts defined: A report on the Keystone Symposium on lipid rafts and cell function, J. Lip. Res. **47**, 1597 (2006).

[32] A. J. García-Sáez, S. Chiantia, and P. Schwille, Effect of line tension on the lateral organization of lipid membranes, J. Biol. Chem. **282**, 33537 (2007).

[33] K. V. Pinigin, O. V. Kondrashov, I. Jiménez-Munguía, V. V. Alexandrova, O. V. Batishchev, T. R. Galimzyanov, and S. A. Akimov, Elastic deformations mediate interaction of the raft boundary with membrane inclusions leading to their effective lateral sorting, Sci. Rep. **10**, 4087 (2020).

[34] M. Hamm and M. M. Kozlov, Elastic energy of tilt and bending of fluid membranes, Eur. Phys. J. E **3**, 323 (2000).

[35] O. V. Kondrashov, K. V. Pinigin, and S. A. Akimov, Characteristic lengths of transmembrane peptides controlling their tilt and lateral distribution between membrane domains, Phys. Rev. E **104**, 044411 (2021).

[36] O. V. Kondrashov, P. I. Kuzmin, and S. A. Akimov, Hydrophobic mismatch controls the mode of membrane-mediated interactions of transmembrane peptides, Membranes **12**, 89 (2022).

[37] W. Rawicz, K. C. Olbrich, T. McIntosh, D. Needham, and E. Evans, Effect of chain length and unsaturation on elasticity of lipid bilayers, Biophys. J. **79**, 328 (2000).

[38] V. Vitkova, P. Méléard, T. Pott, and I. Bivas, Alamethicin influence on the membrane bending elasticity, Eur. Biophys. J. **35**, 281 (2006).

[39] B. Kollmitzer, P. Heftberger, M. Rappolt, and G. Pabst, Monolayer spontaneous curvature of raft-forming membrane lipids, Soft Matter **9**, 10877 (2013).

[40] M. Kaltenegger, J. Kremser, M. P. Frewein, P. Ziherl, D. J. Bonthuis, and G. Pabst, Intrinsic lipid curvatures of mammalian plasma membrane outer leaflet lipids and ceramides, Biochim. Biophys. Acta **1863**, 183709 (2021).

[41] E. Bamberg and P. Läuger, Channel formation kinetics of gramicidin A in lipid bilayer membranes, J. Membr. Biol. **11**, 177 (1973).

[42] K. Lum, H. I. Ingólfsson, R. E. Koeppe, and O. S. Andersen, Exchange of gramicidin between lipid bilayers: Implications for the mechanism of channel formation, Biophys. J. **113**, 1757 (2017).

[43] S. A. Akimov, P. I. Kuzmin, J. Zimmerberg, F. S. Cohen, and Y. A. Chizmadzhev, An elastic theory for line tension at a boundary separating two lipid monolayer regions of different thickness, J. Electroanal. Chem. **564**, 13 (2004).

[44] P. I. Kuzmin, S. A. Akimov, Y. A. Chizmadzhev, J. Zimmerberg, and F. S. Cohen, Line tension and interaction energies of membrane rafts calculated from lipid splay and tilt, Biophys. J. **88**, 1120 (2005).